23rd ABCM International Congress of Mechanical Engineering
December 6-11, 2015, Rio de Janeiro, RJ, Brazil

DYNAMIC ANALYSIS OF A LIQUID ROCKET TURBOPUMP UNIT

Daniel Fraga Sias[1]
danieldfs@iae.cta.br
Everaldo de Barros[2]
everaldoeb@iae.cta.br
Carlos d'Andrade Souto[3]
carloscdas@iae.cta.br
Daniel Soares de Almeida[4]
danieldsa@iae.cta.br
[2,3]Institute of Aeronautics and Space (IAE), Dvivision of Integration and Tests (AIE), São José dos Campos, Brazil
[1,4]Institute of Aeronautics and Space (IAE), Dvivision of Space Propulsion (APE), São José dos Campos, Brazil
[3] Aeronautics Institute of Technology (ITA), São José dos Campos, Brazil

Abstract. *The use of liquid rocket engines in space launchers offers many advantages over its solid counterparts: higher specific impulse; the possibility of re-ignition in flight and the control of thrust vector magnitude. Pressurized tanks or turbopumps are used to inject fuel and oxidizer into the combustion chamber. In order to allow the injection the propellant lines pressure must be higher than the chamber pressure. Since more efficient engines require higher combustion chamber pressure, only turbopumps systems can provide pressure high enough to feed the lines. These systems operate at very high velocities and suffer intense dynamic loads. Therefore its rotor-dynamic behavior must be evaluated during the design stage. In this work a turbopump rotor was modeled numerically by building two finite element models: one with flexible shaft and rigid disks and another with flexible shaft and disks (solid elements). An experimental modal test of the rotor in a free-free stationary condition was performed also. The results for the three analysis were compared and discussed. Finally, the full rotor - bearing system was analyzed and classical rotor-dynamics results like critical speeds and Campbell's diagram were obtained.*

Keywords: *rotordynamics, liquid propellant rockets, finite elements, modal tests.*

1. INTRODUCTION

The needs of more powerful and controllable rockets in space applications leads to liquid propelled engines. Liquid rocket engines allow the control of thrust vector magnitude and more specific impulse (a measure of engine's efficiency given by the impulse per unit mass of propellant used) than solid propelled engines and due this characteristics become very important in the space launcher's industry. Nevertheless, liquid engines are much more technically complex than its solid counterparts.

Until now in Brazilian Space program only solid rocket motors were used. As shown in (Almeida and Pagliuco, 2014), the Institute of Aeronautics and Space (IAE) is currently developing liquid rocket engines technology.

The fuel and the oxidizer need to be injected into the combustion chamber at high pressures. The use of pressurized tanks is the simplest liquid feeding system but also puts short limits to the combustion chamber pressure and consequently the engine's specific impulse. Also, tanks must be strong enough (and consequently heavy) to withstand the internal pressure necessary to expel the propellants (usually provided by some inert gas external tank). Thus, in order to obtain better performances, turbopump units (TPU) need to be used.

In a TPU one (or more) turbine drives fuel and oxidizer pumps. The turbine can be driven by hot gas produced in its own gas generator or by the expansion of fuel used to cool the combustion chamber. An schematic view of a liquid rocket engine with a turbopump is displayed in Fig. (1).

In a real rotor its geometric center and its mass center do not coincide exactly, even for rotors carefully manufactured. Due to this fact an unbalance force appears pushing the rotor outside its geometric center. This force magnitude is proportional to the rotor angular velocity. Since a TPU rotor operates spinning at tens of thousands of rpm, this kind of mechanical systems presents intrinsic transversal vibrations when operating. Thus it is important to evaluate the level of vibrations of a TPU rotor even during the early stages of design.

Numerical models of different complexity are available to simulate a rotor dynamic behavior. In this work two kinds of numerical models were built in order to evaluate the rotor dynamic behavior when spinning. Also an experimental modal analysis was performed for the rotor as a stationary structure. Some classical rotordynamics results like Campbell's diagram, unbalance response and whirling modes shapes were calculated.

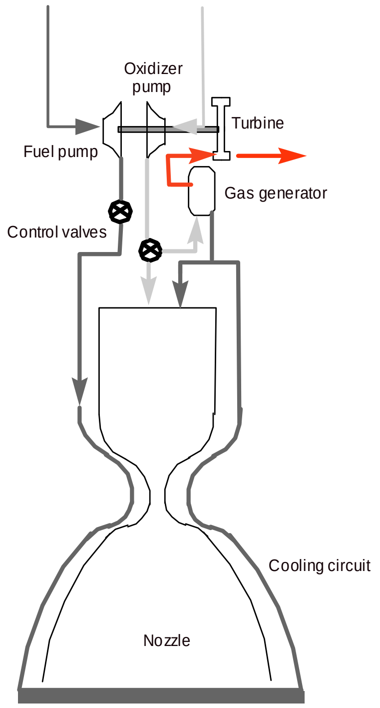

Figure.1 – A liquid rocket engine with turbopump

2. ROTOR MODELS

Three main kinds of numerical models for a rotor-bearing system can be considered.

In the most simple the whole rotor is treated as a rigid body supported by soft bearings. The rotor transversal motions is described by 4 degrees of freedom that can be attached to the center of gravity (horizontal and vertical displacements and pitch and yaw angles) or to two points each one in a rotor tip (horizontal and vertical displacements). This is the rigid rotor model.

In a model with intermediate complexity the shaft is treated as a spinning beam and all disks as rigid bodies. A finite element model with beam elements and point masses and inertias can be built. This is the flexible shaft model.

In a most complete model the disks flexibility is also considered. A finite element model with different kinds of elements can be built. Thisi s the flexible rotor model.

In this study the second and the third models where built and used to analyze the TPU rotor-bearing system.

3 FLEXIBLE SHAFT EQUATIONS

Considering a rotor composed by disks, shaft and bearings with some mass unbalance. Expressions for kinetic energy can be written for the disks, the shaft and the mass unbalance. The same is valid for the strain energy of the shaft. Virtual work of forces due to the bearings can also be evaluated and then its corresponding forces acting on the shaft can be accounted for. Then Lagrange's equation can be written to each component of the rotor:

$$\frac{d}{dt}\left(\frac{\partial T}{\partial \dot{q}_i}\right) - \frac{\partial T}{\partial q_i} + \frac{\partial U}{\partial q_i} = Fq_i \tag{1}$$

where T is the kinetic energy, U the strain energy, q_i are generalized coordinates and Fq_i are generalized forces.

By applying Eq. (1) to each rotor component separately (disks, shaft, bearings and mass unbalance) one can obtain the equations for these components.

Using the finite – element method, a flexible rotor can be modeled by considering its shaft as a beam, its disks as points with mass and inertia and its bearings as horizontal and vertical stiffness (eventually some coupling can be present). Masses unbalance are included in the model as external forces.

3.1.Shaft modelling

The shaft element (an Euler-Bernoulli beam element) with its degrees of freedom can be seen in Fig.(1), extracted from M. Lalanne and G. Ferraris (1990):

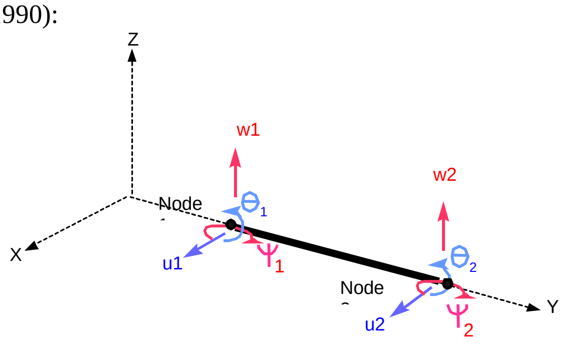

Figure. 2 – Shaft element

The matrix equation for a single shaft element is:

$$\left[M_S^e\right]\left\{\ddot{x}_S^e(t)\right\}-\Omega\left[G_S^e\right]\left\{\dot{x}_S^e(t)\right\}+\left[K_S^e\right]\left\{x_S^e(t)\right\}=\left\{f_S^e(t)\right\} \tag{2}$$

The stiffness matrix can include the effect of axial forces acting on the shaft. The nodal displacement vector is:

$$\delta=\{u_1 \quad w_1 \quad \theta_1 \quad \Psi_1 \quad u_2 \quad w_2 \quad \theta_2 \quad \Psi_2\} \tag{3}$$

3.2. Disks

The matrix equation for a single disk element is:

$$\left[M_d^e\right]\left\{\ddot{x}_d^e(t)\right\}-\Omega\left[G_d^e\right]\left\{\dot{x}_d^e(t)\right\}=\left\{f_d^e(t)\right\} \tag{4}$$

The disk element degrees of freedom are:

$$\delta=\{u \quad w \quad \theta \quad \Psi\} \tag{5}$$

3.3. Bearings The bearings act as supports to the shaft and also add some damping on the system. So they are governed by:

$$\left[C_b^e\right]\left\{\dot{x}_b^e(t)\right\}+\left[K_b^e\right]\left\{x_b^e(t)\right\}=\left\{f_b^e(t)\right\} \tag{6}$$

The bearings nodal displacement vector $\left\{x_b^e(t)\right\}$ is the same as the disk one shown in Eq. (6). For some kinds of bearings the damping and stiffness matrices will be dependant of the shaft angular velocity.

3.4. Rotor

By assembling the equations of all components one can obtain the system's global equations:

$$[M]\{\ddot{x}(t)\}+[D(\Omega)]\{\dot{x}(t)\}+[K]\{x(t)\}=\{f(t)\} \tag{7}$$

Where [*M*] is the mass matrix, [*D(Ω)*] is given by $[D(\Omega)]=([C]-\Omega[G])$, [C] is the damping matrix, [G] the giroscopic matrix and is, [*K*] is the stiffness matrix, {*x(t)*} is the nodal displacements vector and {*f(t)*} is the nodal force vector. The mass matrix is symmetric and invariant, the giroscopic matrix is skew symmetric. Depending on the bearings nature, the stiffness matrix can be considered symmetric and invariant (in the case of ball bearings, e.g.).

The shaft, disks and bearings elementary matrices can be obtained in (Nelson & McVaugh, 1976) or in text books of rotordynamics like (Lalanne & Ferraris,1990) and (Childs 1993).

4 FLEXIBLE ROTOR EQUATIONS

For this model the Eq.(7) applies but its matrices now describes the whole rotor structure. The bearings influence can be accounted for by including discrete springs connected to some rotor nodes and do the rotor case/foundations or by applying structural boundary conditions to some rotor nodes.

5 SYSTEM STUDIED

A view of the turbopump unit rotor analyzed is displayed in Fig. (3), extracted from (Almeida and Pagliuco, 2014). It is similar to the system analyzed in (Porto, 2011). It has two pumps, a turbine (the bigger disc) and two roller bearings.

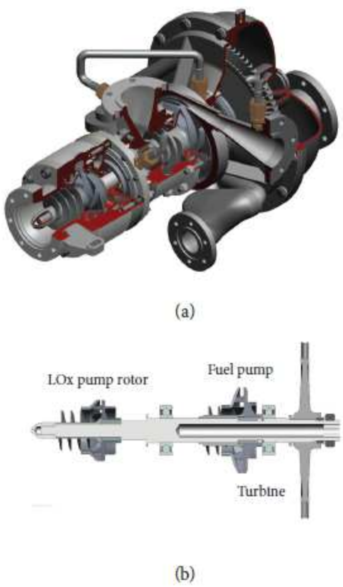

Figure.3 – A turbopump unit
(a) Turbopump in its case (b) Turbopump rotor

A rotor with the same pyhsical properties of the designed one (but with discs in the place of the pumps and turbine) was manufactured in stainless steel AISI 410 (Young's modulus 200 GPa, specific mass 7800 Kg/m^3). Due to confidentiality the physical properties are not listed. The shaft modeled can be seen in Fig. (4). The bearings stiffness and damping coefficients were the same used in (Souto, 2011) and are listed in Tab. (1). The cross terms were assumed as zero.

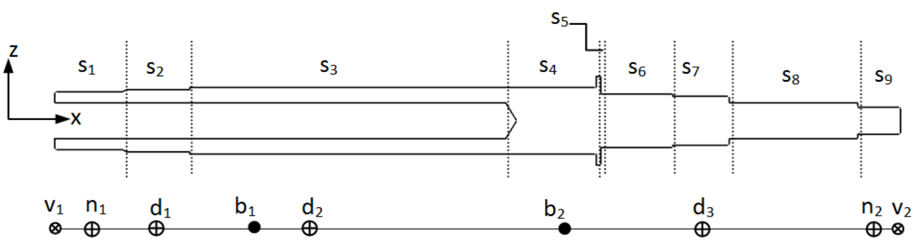

⊕ - Discs and nuts
● - Bearings
⊗ - Ends of the shaft

Figure 4 – Shaft with discs and bearings positions

Table 1- Bearings stiffness and damping coefficients

Elementos	K_{yy} [N/m]	K_{zz} [N/m]	C_{yy} [Ns/m]	C_{zz} [Ns/m]
b_1, b_2	25.48×10^6	25.48×10^6	0.5×10^3	0.5×10^3

6 ANALYSIS PERFORMED

6.1 Experimental modal analysis of the stationary rotor

The rotor tested in a free-free condition can be seen in Fig. (5). The modal testing was performed by applying a random excitation and using a Hanning window. The frequency band analyzed was from 0 to 6400 Hz with a frequency resolution of 0.25 Hz. A more detailed description of the modal test was presented in (Barros, 2013).

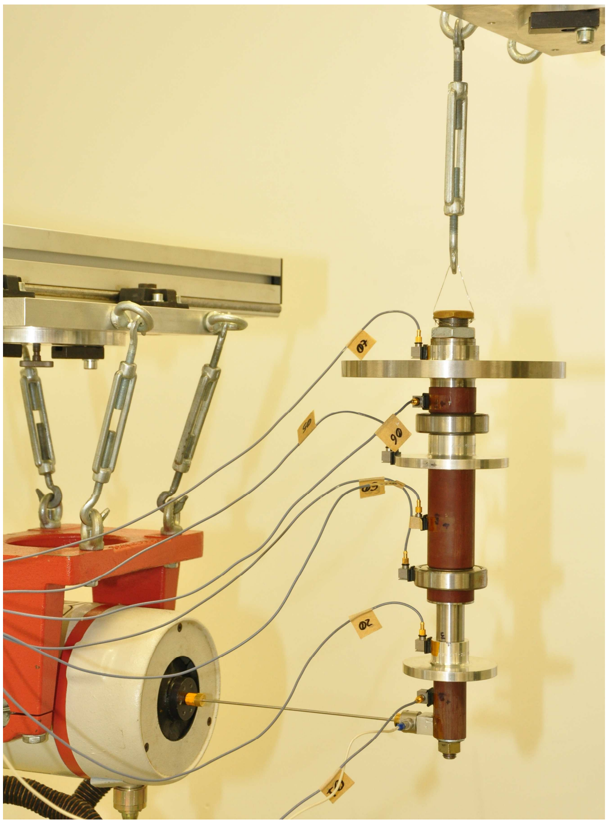

Figure 5– Rotor tested instrumented

6.2 Numerical analsysis

All the analysis were performed by using the open source software Salome-Meca (pre and post processors) and Code Aster (solver). The shaft was modeled by using tridimensional linear frame elements with 2 nodes. Each node has 6 degrees of freedom (3 translational and 3 angular]).

In the solid model quadratic tethraedral elements with 10 nodes with 3 translational degrees of freedom per node.

6.21 Flexible shaft model

The flexible shaft was discretized by using 36 frame elements and 37 nodes. The discs (turbine, fuel and oxidizer pumps) were modeled by using point masses with the same mass and inertia properties.

6.2.2 Flexible rotor model

This model can take into account the discs flexibility. The rotor mesh had 58414 elements.

7 RESULTS AND DISCUSSION

7.1 ROTOR AT REST IN FREE-FREE CONDITION

The FEM (beam and solid models) and experimentally results for the free-free condition are displayed in Tab.(2). In order to allow a comparison among all three analysis only shaft flexure modes were considered. Due to the rotor symmetry some modes have very close frequencies. In mode 5 the shaft presented longitudinal displacements and therefore was not identified in the modal test. One can realize that the beam model give frequencies closer to the experimentally obtained ones than the solid model.

Table 2 – Results for the free-free condition

Flexure modes	f_n [Hz]$_{beam}$	f_n [Hz]$_{3D}$	f_n [Hz]$_{exp}$/damping	Diference (beam-3D)	Diference (beam-exp)
1	575.241	627.36	574.46/0.44	-9.06 %	0.13 %
2	575.268	627.38	-		
3	1213.89	1369.64	1031.56/1.67	-12.83 %	17.68 %
4	1213.95	1369.89	-		
5	1692.48	1896.60	-		
6	2226.30	2500.54	2205.75/3.07	-12.32 %	0.93 %
7	2226.33	2501.29	-		

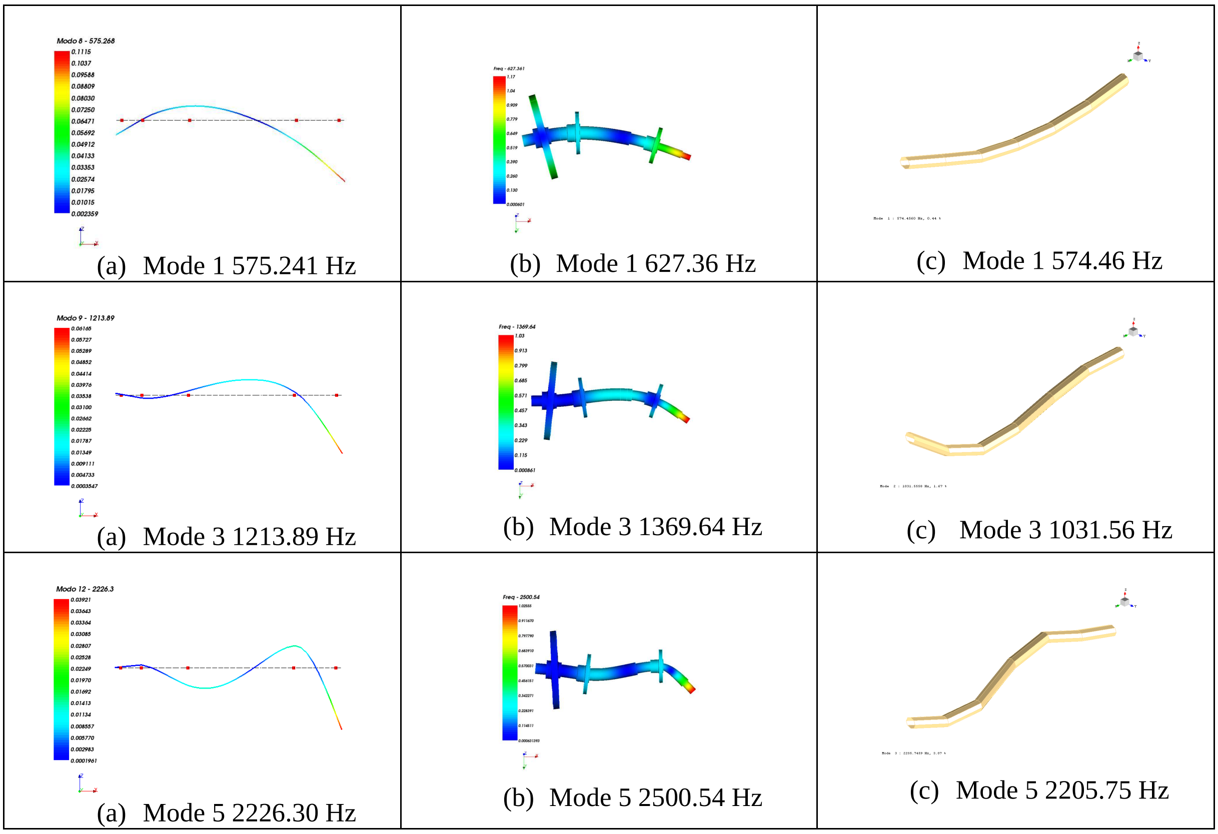

(a) Mode 1 575.241 Hz
(b) Mode 1 627.36 Hz
(c) Mode 1 574.46 Hz
(a) Mode 3 1213.89 Hz
(b) Mode 3 1369.64 Hz
(c) Mode 3 1031.56 Hz
(a) Mode 5 2226.30 Hz
(b) Mode 5 2500.54 Hz
(c) Mode 5 2205.75 Hz

Figure 6 – Rotor mode shapes for free-free condition obtained from: (a) FEM results beam model; (b) FEM results solid model; (c) modal tests

7.2 ROTORDYNAMIC RESULTS

The Campbell diagram and the critical speeds were obtained by using the Code Aster software to analyze the rotor beam model supported by the bearings whose properties were listed in Tab. (1). The Campbell diagram for this configuration is displayed in Fig. (7). Its respective critical speeds are listed in Tab. (3). The critical speed value marked with bold numbers corresponds to a forward whirl mode.

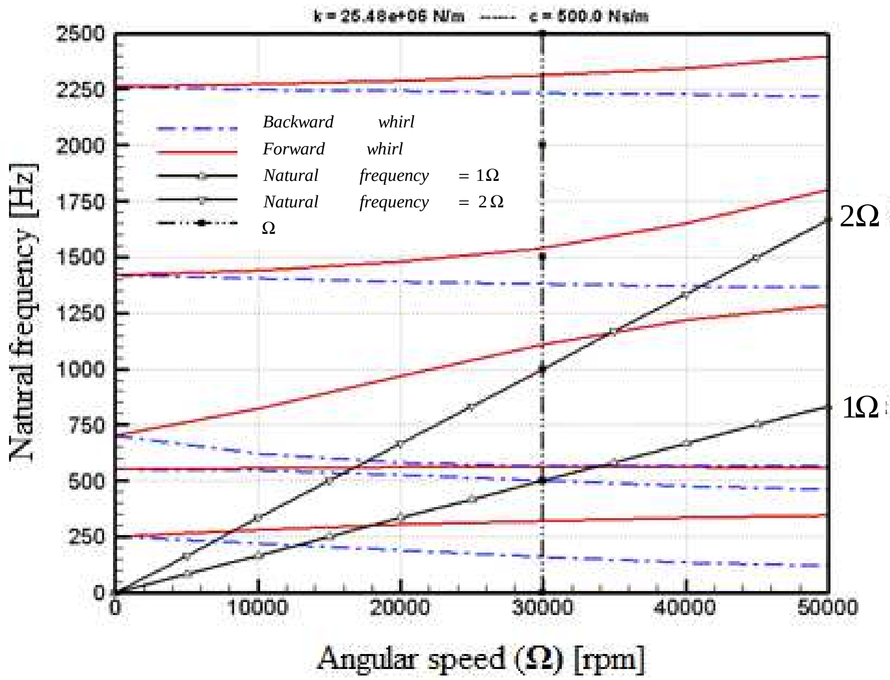

Figure 7 – Campbell's diagram

Table 3 – Critical speeds

Modes	Critical speeds [rpm]	Natural Frequency [Hz]
1	12675.02	211.25
2	**17941.86**	299.03
3	29922.60	498.71
4	33824.63	563.74
5	33827.36	563.79

The turbopump operational speed is 29985 rpm. As can be seen in Fig. (7) and Tab.(3), a backward whirl critical speed is very close to this value. In order to avoid this critical speed it was suggested in (Sias, 2013) to change the bearings stiffness. Another analysis was performed with the bearing stiffness changed to 55.48×10^6 N/m. Its results are displayed in Fig. (8) and Tab.(4). It can be noticed that the new bearing stiffness gives a much better operational condition far from any critical speed.

8 CONCLUSIONS AND FUTURE DEVELOPMENTS

The dynamic behavior of the rotor to be used in the turbopump unit of the L75 liquid rocket engine was evaluated numerically and experimentally in a free-free condition. Two kinds of finite elements models were built, a flexible shaft with rigid discs (beam + point masses) and a flexible shaft and discs (with solid elements). The flexible shaft with rigid discs shown a better agreement with the modal tests.

By using the flexible shaft with rigid discs model a rotordynamic analysis was conducted evaluating the behavior of the rotor-bearing system. This analysis indicates a critical speed very close to the operational speed. Another analysis was carried out with stiffer bearings. In the second configuration the critical speeds become far from the operational angular speed.

All numerical analysis were performed using open source programs (Salome –Meca pre and post processor and Code Aster solver).

This work is based on two reports (Sias, 2013 and Barros, 2013) written before the project L75 suffer some modifications due to the changing in the fuel from kerosene to ethanol. These modifications altered the turbopump characteristics and so further analysis shall be performed.

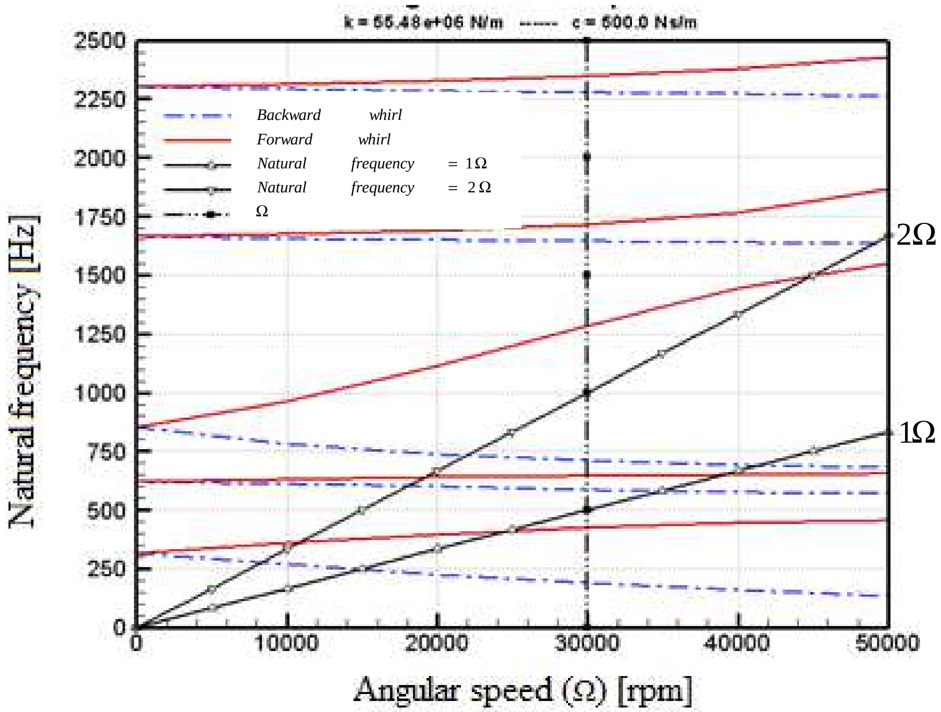

Figure 8 – Campbell's diagram

Table 4 – Critical speeds (2nd configuration)

Modes	Critical speeds [rpm]	Natural Frequency [Hz]
1	14828.31	247.14
2	**24574.94**	409.58
3	34962.54	582.71
4	39076.86	651.28
5	41477.70	691.29

9 REFERENCES

Almeida, D. S. and Pagliuco, C. M. M., "Development Status of L75: A Brazilian Liquid Propellant Rocket Engine", *Journal of Aerospace Technology and Management, JATM, Vol.6, No 4, pp.475-484, Oct.-Dec., 2014*

Barros, E. "Relatório de ensaio de análise modal experimental do modelo de balanceamento da TPU para o L75", RE 069/AIE/2013, *IAE internal report*, São José dos Campos: 2013, in Portuguese

Childs, D. *Tubomachinery Rotordynamics - Phenomena, Modeling and Analysis* New York: J. Wiley & Sons: 1993

Lalanne, M. & Ferraris, G. *Rotordynamics Prediction in Engineering* Chichester: John Wiley and Sons: 1990

Nelson, H.D. & McVaugh, J. M. "The dynamics of rotor bearing systems using finite-elements" *Transactions of ASME: Journal for Engineering for Industry*, p.593-600, may 1976

Porto, B. F. *Projeto do conjunto rotor de uma turbobomba de um motor foguete de propulsão líquida de 75 KN de empuxo* Master' deg'ree dissertation, ITA, São José dos Campos: 2011, in Portuguese.

Souto, C.,d'Andrade "Análise Dinâmica para Turbobomba do Motor Foguete a Propulsão Líquida L75", RT 006/AIE/R/2011, *IAE internal report*, São José dos Campos: 2011, in Portuguese

Sias, D. F. "Análise modal e rotodinâmica do modelo de balanceamento da turbobomba do motor L75" ", RT 007/APE/R/2013, *IAE internal report*, São José dos Campos: 2013, in Portuguese

10 RESPONSIBILITY NOTICE

The authors are the only responsible for the printed material included in this paper.